The FASEB Journal express article 10.1096/fj.04-1642fje. Published online August 2, 2004.

Inhibition of p38 MAP kinase- and RICK/NF-κB-signaling suppresses inflammatory bowel disease

Eike Hollenbach,[*,†,§] Manfred Neumann,[*,§] Michael Vieth,[‡] Albert Roessner,[‡] Peter Malfertheiner,[†,¶] and Michael Naumann[*,¶]

*Institute of Experimental Internal Medicine; [†]Department of Gastroenterology, Hepatology and Infectiology; and [‡]Institute of Pathology Otto-von-Guericke-University, Magdeburg, Germany

Corresponding author: Michael Naumann, Institute of Experimental Internal Medicine Otto-von-Guericke-University Leipziger Strasse, 44 D-39120 Magdeburg, Germany. E-mail: naumann@medizin.uni-magdeburg.de

[§]These authors contributed equally to this work.

[¶]These authors share senior authorship.

ABSTRACT

Ulcerative colitis and Crohn's disease are the two entities of chronic inflammatory bowel diseases (IBD). One of the main pathogenic mechanisms is probably a dysregulated immune response triggered by products of the enteric bacterial flora. The goal of this study was to evaluate the effects of the p38 mitogen-activated protein kinase (MAPK) inhibitor SB203580 on inflammatory responses using the DSS-induced experimental colitis model in mice reflecting human IBD. We found that SB203580 improved the clinical score, ameliorates the histological alterations, and reduces the mRNA levels of proinflammatory cytokines. In addition to p38 kinase activity, the "classical" and the "alternative" NF-κB pathways were also strongly activated during colitis induction. All three pathways were drastically down-regulated by SB203580 treatment. An analysis of the molecular basis of NF-κB activation revealed that Rip-like interacting caspase-like apoptosis-regulatory protein kinase (RICK), a key component of a pathway leading to NF-κB induction, is also strongly inhibited by SB203580. Since RICK is an effector kinase of NOD2, an intracellular receptor of bacterial peptidoglycan, these results support the notion that NOD signaling could play a pivotal role in the IBD pathogenesis. Thus, RICK could represent a novel target for future therapies in human IBD.

Key words: IBD • IκB • Rip-like interacting caspase-like apoptosis-regulatory protein kinase

Ulcerative colitis and Crohn's disease are inflammatory bowel diseases (IBD) of unknown etiology characterized by chronic relapsing inflammation of the gastrointestinal tract due to a dysregulated mucosal immune response (1). Beside a genetic predisposition and environmental factors (1–2), either nonpathogenic intestinal flora or nonidentified pathogenic bacteria seem to play a pivotal role during the initiation process of inflammation (3–6).

Dextran sulfate sodium (DSS)-induced colitis in mice shows reproducible morphological changes, which are very similar to those seen in patients with ulcerative colitis. These

pathologies include predominant left-sided colonic inflammation, prominent regeneration of the colonic mucosa cells with dysplasia leading to colon cancer, shortening of the large intestine, focal crypt damage, and frequent lymphoid hyperplasia in both biological systems (7, 8). DSS induces primary effects on epithelial cells and has been shown to inhibit the proliferation and regeneration of mouse epithelial cells in vitro (8). This enables the contact between cells of the innate immunity with bacteria of the bowel (8, 9), an event that has been proposed to be a crucial initiation step in the pathogenesis of human IBD (3, 6).

On the molecular level, p38 is assumed to be a major mediator of inflammation in IBD (10). p38 is a member of the mitogen-activated protein kinase (MAPK) family, which are ubiquitously expressed serine-threonine kinases playing important roles in various signal transduction pathways in mammalian cells (11, 12). p38 becomes activated during treatment of cells with proinflammatory cytokines, such as interleukin 1β (IL-1β), tumor necrosis factor-α (TNF-α), transforming growth factor-β (TGF-β), as well as CD40 ligand (13). It has been demonstrated that p38 mediates phosphorylation of transcription factors, thereby regulating gene expression and the induction of cytokine production (14). p38 is activated by dual phosphorylation on Thr180 and Tyr182 by the upstream MAPKs MKK3 and MKK6. MKK3 is especially important for TNFα-induced p38 activation (15) and for the p38-mediated synthesis of IL-12 and IFN-γ (16), key cytokines in the pathogenesis of IBD.

The p38 gene has been localized to the major IBD susceptibility region 3 on chromosome 6 (10, 17, 18). A role for p38 as an IBD susceptibility gene has not yet been proven since there are other candidate genes that may ultimately explain a genetic association to this IBD locus. p38α shows the strongest increase in kinase activity among the MAPKs within the inflamed intestinal mucosa of IBD patients (10, 19). Thus, p38 has been suggested to play a key role in intestinal inflammation, cytokine production, and T cell activation in IBD (20). Various animal models suggest that p38 inhibitors such as SB203580 attenuate disease activity, mortality or reduced—at least partially—proinflammatory cytokine concentrations (21–23). Therefore, p38 is a promising candidate for targeted inhibition in acute and chronic inflammation. Recently, a pilot study investigating the efficacy of the combined p38 and JNK inhibitor CNI-1493 in patients with Crohn's disease showed indeed a significant clinical improvement in moderate to severe active disease (19).

NOD2 is presently the only independently confirmed susceptibility gene linked to CD (24, 25). The NOD2 protein is a key component of the innate immune system and encodes an intracellular receptor for bacterial peptidoglycan (26). Carriers of mutations in the NOD2 gene have an up to 42-fold increased risk in developing Crohn's disease (24, 25). NOD2 mutations are predisposing for a more youthful onset of Crohn's disease (27) and a relation between NOD2 genotype and phenotype of Crohn's disease and recently of ulcerative colitis was noted (28, 29). The clearance of *Salmonella typhimurium* is highly increased in cells expressing wild-type NOD2, whereas cells transfected with mutated NOD2, as detected in patients with Crohn's disease, were unable to clear the bacteria (30). Further, in vitro studies have demonstrated the functional importance of NOD signaling for induction of NF-κB activation (30).

The transcription factor NF-κB plays a pivotal role in the regulation of immune response, apoptosis, and inflammation (31). NF-κB is a homo- or heterodimer consisting of p65 (RelA),

RelB, c-Rel, p50, and p52 in almost any combination. The classical pathway of NF-κB activation induced by multiple proinflammatory signals proceeds through IκB kinase (IKK)-mediated phosphorylation of cytoplasmic NF-κB inhibitors, the IκBs. This site-specific phosphorylation is a prerequisite for IκB ubiquitination and the subsequent degradation of this inhibitor by the 26S proteasome. Recently, an alternative activation pathway for NF-κB, based upon the NF-κB inducing kinase (NIK)/IKKα-dependent processing of p100 to p52 was described (32–34). This pathway preferentially leads to the formation of p52/RelB heterodimers, which are important for adaptive immunity, synthesis of homing chemokines, and for the normal development of lymphoid organs (35, 36). In particular, RelB seems to control inflammatory responses, since RelB-deficient mice display a phenotype with multiorgan inflammation and multifocal defects in the immune response (37, 38).

In this study, we investigated the impact of the p38 inhibitor SB203580 using a murine DSS-induced colitis model of increasing and resolving inflammation in vivo. SB203580 inhibited p38 activity as well as the classical and alternative pathways of NF-κB activation. We demonstrate that RICK is a molecular target of SB203580. The inhibition of RICK is probably the main mechanism of NF-κB inhibition by SB203580, resulting in decreased levels of proinflammatory cytokines in the bowel. Thus, we identified RICK as a new target for the treatment of IBD.

MATERIALS AND METHODS

Animals and induction of colitis

Female BALB/c mice (6–8 weeks old) ~19–22 g in body weight were obtained from Harlan-Winkelmann (Borchen, Germany) and given ad libitum access to water and standard rodent food. Mice were weighted and randomized into groups of 7. Clinical assessments and histological scoring of colitis were performed in a blinded fashion. Experiments were performed after ≥3 days following arrival of the animals. Colitis was induced by replacing normal drinking water with water containing 3% DSS (molecular weight 40 kD; Sigma, Deisenhofen, Germany) for 7 days as indicated. DSS supplementation was stopped after day 7. Treatment with 5 μmol SB203508/kg body weight in 200 μl 0.9% NaCl solution was given i.p. twice daily beginning 60 h after DSS treatment and continuing until death. For control experiments, bowel tissue was analyzed from (1) completely untreated animals, (2) animals receiving vehicle injections (3% DMSO), or (3) mice receiving SB203580 (Calbiochem, Schwalbach, Germany) injections in the same manner, respectively.

Clinical and histological analysis

Daily weight, physical condition, stool consistency, water/food consumption, and the presence of gross and occult blood in excreta and at the anus were determined (Haemocare, Care Diagnostics, Vörde, Germany). The colitis score was calculated by assigning scores of these parameters resulting in the disease activity index (DAI), according to the system of Hartmann et al. (39). The following parameters were used for calculation: 1. weight loss (0 points=0% weight loss from baseline, 1 point=1–5% weight loss, 2 points=5–10% weight loss, 3 points=10–20% weight loss, 4 points=more than 20% weight loss); 2. stool consistency (0 points=normal, 2 points=pasty/semiformed stool that did not adhere to the anus, 4 points=liquid); 3. bleeding (0

points=negative hemoccult test, 2 points=positive hemoccult test, 4 points=gross bleeding). The sum of this score was divided by three resulting in the total DAI ranging from 0 (healthy) to 4 (maximal activity of colitis). Animals were killed by CO_2 inhalation at day 3, 5, 7, 10, and 13 (n=7 in each group per day). After sacrifice, the colon was quickly removed, opened longitudinally, and gently cleared of stool. Subsequently, samples of colonic tissue were either fixed in 4% buffered formalin, embedded in paraffin and 4-μm-thick serial step sections were stained with hematoxylin-eosin (HE) or snap-frozen in liquid nitrogen in OCT embedding medium and stored at –80°C until usage. Histological scoring was performed semiquantitatively in HE stained sections as described by Dieleman et al. (40), grading inflammation (0 points=none to 3 points=severe), extent (0 points=none to 3 points=transmural), regeneration (0 points=complete regeneration or normal tissue to 4 points=no tissue repair), crypt damage (0 points=none to 4 points=entire crypt and epithelium lost), and multiplied by the involvement, respectively (0 points=none to 4 points=76–100%).

Blood sampling

Blood (~0.4 ml) was drawn intracardially and mixed with 50 μl of 0.5 M EDTA. Blood samples were subjected to differential blood cell count analysis.

Extraction of total RNA and quantitative RT-PCR

A gut specimen obtained 5 cm proximal to the anus was used for extraction of total RNA using a recently described method (41). For each animal, 1 μg of total RNA was transcribed into cDNA. Quantitative real-time RT-PCR was performed in an iCycler (BioRad, Munich, Germany). The 30 μl reaction mixture consisted of 15 μl HotStarTaq™ Master Mix, 1.2 μl of the RT-reaction, 0.3 μl SYBR-Green I (1:10000; Molecular Probes, Eugene, OR USA), and 0.5 μM of the specific primers (TIB Molbiol, Berlin, Germany). Initial denaturation and activation of Taq-polymerase at 95°C for 15 min was followed by 40 cycles consisting of 1) denaturation at 94°C for 30 s, 2) annealing at 60°C for 45 s for β-actin, TNF-α, IFN-γ, IL-1β, IL-2, IL-4, IL-12p35, IL-18, at 55°C for IL-10, and at 66°C for IL-12p40), and 3) elongation at 72°C for 30 s. The fluorescence intensity of the double-strand specific SYBR-Green I, reflecting the amount of actually formed PCR-product, was read real-time at the end of each elongation step. Specific initial template mRNA amounts were calculated by determining the time point of a standard curve (artificial units). β-actin mRNA amounts were used to normalize the cDNA contents of the different samples. In addition, an aliquot of the PCR reaction mixture was separated on a 1.8% agarose gel and stained with ethidium bromide.

The following primers were used for the RT-PCR analysis: β-actin: forward primer (fw): TGGAATCCTGTGGCATCCATGAAAC, reverse primer (rev): TAAAACGCA GCTCAGTAACAGTCCG; TNF-α: fw: GGCAGGTCTACTTTGGAGTCATTGC, rev: ACATTCGAGGCTCCAGTGAATTCGG; IFN-γ: fw: AGCGGCTGACTGAACTCAGA TTGTAG, rev: GTCACAGTTTTCAGCTGTATAGGG; IL-1β: fw: TCATGGGATG ATGATGATAACCTGCT, rev: CCCATACTTTAGGAAGACACGGATT; IL-2: fw: TGATGGACCTACAGGAGCTCCTGAG, rev: GAGTCAAATCCAGAACATGCCGC AG; IL-4: fw: CGAAGAACACCACAGAGAGTGAGCT, rev: GACTCATTCATGGTGC AGCTTATCG; IL10: fw: ACCTGGTAGAAGTGATGCCCCAGGCA, rev: CTATGCAG

TTGATGAAGATGTCAAA; IL12p35: fw: GCAAGAGACACAGTCCTGGG, rev: TGCATCAGCTCATCGATGGC; IL12p40: fw: GAGGTGGACTGGACTCCCGA, rev: CAAGTTCTTGGGCGGGTCTG; IL18: fw: GCAAGCTTCGCTCTTCTGTCTACTGA ACTTCGG, rev: GCTCTAGAATGAGATAGCAAATCGGCTGACGG.

Protein extraction from the gut

For total protein preparation, gut specimens obtained 3–4 cm proximal from the anus were snap-frozen in liquid nitrogen and stored at −80°C until extraction of protein. Specimens were homogenized in 1 ml ice-cold lysis buffer containing 0.5% Nonidet P40 (Sigma), 0.5% Triton ×100, 10% (v/v) glycerol, 50 mM TRIS (pH 7.5), 5 mM EDTA, 0.1 M NaCl, 10 mM K_2HPO_4, 0.5% deoxycholic acid (DOC, Sigma), 20 mM NaF, 0.1 mM PMSF, 20 mM glycerol-2-phosphate (Sigma), 1 mM Na_3VO_4, and protease inhibitor cocktail (Boehringer/Roche, Mannheim, Germany). The lysate was centrifuged (14.000 rpm, 4°C) for 15 min and the supernatant was transferred to a new tube. Total protein content was analyzed using the Advanced™ protein assay (Tebu, Offenbach, Germany). Finally, samples were aliquoted and stored at −80°C until usage.

For the cellular subfractionation of proteins, tissue was carefully homogenized so that many viable single cells were obtained and resuspended in 1 ml ice-cold TBS buffer, centrifuged (10 min, 800 g, 4°C), and washed in buffer A (10 mM HEPES pH 7.9, 10% glycerol, 10 mM KCl, 0.1 mM EDTA, 0.1 mM EGTA, 1 mM DTT, 0.5 mM PMSF, 1 mM Na_3VO_4, 10 mM NaF, protease inhibitor cocktail). After centrifugation, the pellet was resuspended in 0.2 ml buffer A and 2 µl 12.5% (v/v) Nonidet P40 was added, briefly incubated on ice, and centrifuged (10 min, 800 rpm, 4°C). The supernatant was used for cytoplasmic analyses. The pellet was washed again in buffer A. After centrifugation, pellets were resuspended in 40 µl buffer C (20 mM HEPES pH 7.9, 400 mM KCl, 1 mM EDTA, 1 mM EGTA, 1 mM DTT, 1 mM PMSF, 1 mM Na_3VO_4, 10 mM NaF, protease inhibitor cocktail) and incubated on a shaker for 1 h at 4°C. Subsequently, samples were centrifuged (10 min, 13,000 g, 4°C), the supernatant (nuclear protein extract) was transferred to liquid nitrogen, and stored at −80°C until usage.

SDS-PAGE and immunoblotting

Protein concentrations were determined for all whole cell, cytoplasmic, and nuclear extracts, and proteins were analyzed by SDS-PAGE and immunoblotting as described previously (42). Immunoblots were developed using enhanced chemiluminescence (ECL, Amersham-Pharmacia Biotech, Inc., Piscataway, NJ) according to the manufacturer's instructions. Since ERK1/2 expression was unchanged during the course of inflammation, ERK1/2 was chosen as a loading control. The following antibodies were used to detect the respective proteins: ERK1/2, p38, and p65 (Santa Cruz Biotechnology, Santa Cruz, CA, USA), phospho-IKKα (Cell Signaling, Frankfurt, Germany), p52 and p100 (Upstate/Biomol, Hamburg, Germany), and RICK (Abcam, Cambridge, MA, USA).

Immunofluorescence microscopy

To identify the cell types where p38 and MKK 3/6 are activated, immunohistochemical studies were performed using gut specimen obtained 3–4 cm proximal to the anus. Cryosections were

fixed in acetone for immunofluorescence microscopy. After washing in PBS, nonspecific binding was blocked with 1% bovine serum albumin (BSA) for 1 h before the addition of primary antibody. Rabbit phospho-p38 antibody or phospho-MKK 3/6 antibody (10 μg/ml, respectively) were added to the slides and incubated for 1 h at room temperature in a humid chamber, respectively. Sections were incubated with 1 μg/ml rabbit IgG as a negative control. After repeated washing with PBS, the sections were incubated with a FITC-conjugated goat anti-rabbit antibody for 1 h. The sections were washed again in PBS and mounted in Vectashield media (Vector Labs, Burlingame, CA, USA).

In vitro kinase assays

RICK and p38 activity were analyzed in an in vitro kinase assay using 0.2 mg protein of lysate incubated with anti-RICK or anti-p38 antibodies (1 μg/sample) by permanent shaking for 3 h at 4°C, respectively. Immune complexes were recovered using 50 μL of a 50% protein A-Sepharose bead suspension (Amersham Biosciences, Braunschweig, Germany) and incubated for 90 min at 4°C in a permanent shaker. Subsequently, immunoprecipitates were washed six times in the same lysis buffer and incubated with 1.5 μg of myelin basic protein (MBP) for the RICK-assay or 1.5 μg ATF-2 for the p38-assay in 20 μl kinase buffer (20 mM HEPES pH 7.6, 2 mM EGTA, 20 mM $MgCl_2$, 1 mM Na_3VO_4, 1 mM DTT, 0.1% Triton X-100, 0.25 mM ATP) for 30 min at 30°C. Samples were suspended in loading buffer and subjected to SDS-PAGE. ATF-2 and the antibody against phospho-ATF-2 were obtained from Cell Signaling (Frankfurt, Germany). Dephosphorylated MBP and antibody against phospho-MBP were purchased from Upstate/Biomol (Hamburg, Germany).

Statistical analysis

The data are expressed as mean values ± SE. Significant differences among treatment groups and controls were assessed by ANOVA and a Bonferroni-Dunn procedure as a post hoc test. Statistical significance of the difference between drug-treated and vehicle-treated groups was established at a probability of $P < 0.05$.

RESULTS

SB203580 reduces the disease activity index of DSS-induced colitis in mice

Initial studies using MAPK-inhibitors like SB203580 in patients with IBD refractory to standard medication were very promising, since most patients showed clinical improvements and were still in clinical and histological remission after six months (19). We were interested in studying the molecular mechanisms of this therapeutic effect in an animal model for intestinal inflammation. The well-established murine model of DSS-induced colitis (7) is commonly used to screen pharmacological agents (8). The disease activity index (DAI) provides a well-characterized scoring system to quantify disease severity that correlates with histological healing (43). Treatment of mice with SB203580 was started 60 h after DSS supplementation when the first signs of colitis were notable. The maximum of colonic inflammation developed at day 7 according to the DAI and the progression of colitis was markedly reduced by SB203580 treatment as reflected by a lower DAI (Fig. 1*A*). After termination of DSS administration (day 7), clinical parameters slowly improved in animals not receiving SB203580 treatment. This

improvement was markedly enhanced in SB203580 treated animals (Fig. 1*A*). Both, control animals without DSS treatment receiving either no (n=10) or peritoneal vehicle (3% DMSO) injections at the same time points as the SB203580 treated animals (n=10) showed no signs of colitis and were therefore considered as one group. Analysis of weight loss, daily food and water consumption revealed a significantly reduced intake of food from day 7 to day 10 in nontreated vs. the SB203580-treated mice. As a consequence, these mice also had a lower weight reduction (Fig. 1*B*).

Differential white blood cell count revealed a dramatic increase of monocytes and granulocytes in the peripheral blood after induction of colitis starting at day 5 with a maximum at day 7. Monocytes were significantly reduced between day 5 and 13 in the SB203580-treated animals, whereas peripheral granulocytes were significantly higher in nontreated mice (Fig. 1*C*).

SB203580 reduces the histological disease score of DSS-induced colitis in mice

Next, we evaluated the histological parameters of experimentally induced colitis and the effects of SB203580 (7 animals/day/treatment group). Treatment of mice with DSS produced a mild colitis after three days with multiple erosive lesions and inflammatory cell infiltrations. The maximum of colitis with ulcerative lesions was notable after seven days (Fig. 2*A*, upper panel). SB203580 treatment clearly reduced the impairment of the glandular architecture and the infiltration of macrophages, lymphocytes, and occasional eosinophils and neutrophils between day 3 and 7 (Fig. 2*A*, lower panel). Starting at day 3, the histological signs of colitis as reflected by a lower histological score were reduced in SB203580-treated mice (Fig. 2*B*). The resolution of inflammation was significantly faster in the SB203580-treated group after discontinuing DSS feeding.

SB203580 inhibits pro-inflammatory cytokines

The cytokine profile is the decisive parameter of any inflammatory process. Cytokine synthesis is regulated by p38 and other signaling pathways. Thus, we examined the mRNA expression of TNF-α, IFN-γ, IL-2, IL12-p35, IL-18, and IL-10 in the bowel tissue (7 animals/day/treatment group) using real-time quantitative PCR. These experiments showed that mRNA concentrations of proinflammatory cytokines strongly increased at day 3 and reached a maximum at day 7 (IFN-γ, IL-18, and IL-12 p35) or at day 10 (TNF-α). SB203580 drastically down-regulated mRNA levels of these cytokines (Fig. 3).

Only a moderate increase was notable for the mRNA level of IL-2, which was not significantly suppressed by SB203580. In contrast, SB203580 significantly up-regulated the anti-inflammatory cytokine IL-10 between days 5 and 10 after colitis induction (Fig. 3). Treatment with SB203580 alone in control animals had no discernible effect compared with vehicle treatment.

SB203580 inhibits p38 activity in mononuclear and plasma cells of the lamina propria

Using phospho-specific antibodies, we analyzed the activity of p38 MAPK, as well as the upstream kinases MKK3/6 in inflamed bowel tissue by immunofluorescence microscopy. p38 (Fig. 4*A*) and MKK3/6 (data not shown) were only activated in mononuclear and plasma cells of

the lamina propria. In general, the severity of inflammation detected by immunohistological analysis correlated with the clinical score in SB203580-treated and nontreated animals. No lesions or signs of inflammation were observed in control mice.

SB203580 targets only the ATP binding of p38 but does not interfere with p38 phosphorylation (44). To correctly assess the activity of p38, we immunoprecipitated this MAPK from bowel tissue protein extracts and performed an in vitro kinase assay using ATF-2 as a substrate followed by immunoblotting with phospho-specific ATF-2 antibodies. A strong increase of p38 activity was detected after day 3 with a maximum between days 5 and 10. This activity was strongly inhibited by SB203580 during the course of colonic inflammation (Fig. 4*B*).

SB203580 inhibits the classical and alternative NF-κB pathways

In addition to p38, NF-κB is an important regulator of genes encoding cytokines and their receptors. SB203580 inhibited these cytokine genes in murine bowel tissue. Therefore, we wanted to examine whether SB203580 had also an effect on NF-κB activation in our animal model of intestinal inflammation. Cytoplasmic and nuclear extracts were prepared from bowel tissue. First, we analyzed the phosphorylation of IKK, IκBα degradation, and the nuclear translocation of p65 by immunoblot analysis. These parameters served as a readout for NF-κB activation. We found a statistically significant peak of IKKα/β-phosphorylation and of IκBα-degradation at day 7 after the start of DSS feeding (Fig. 5*A*). In addition, nuclear translocation of p65 showed the same kinetics as IκBα degradation (Fig. 5*B*). Both observations indicate a maximal NF-κB activation at days 5 to 7. Surprisingly, SB203580 inhibited IκBα degradation and p65 translocation, respectively, indicating that SB203580 is not only specific for p38 MAPK but has also other targets involved in NF-κB activation.

We further analyzed the alternative pathway of NF-κB activation involving p100 processing to active p52. We performed immunoblot analysis using antibodies recognizing both, the p100 precursor as well as the p52 product. This NF-κB activation pathway was also activated during DSS-induced colitis. Furthermore, the p100 processing was strongly blocked by SB203580 treatment (Fig. 5*C*). This indicates that SB203580 has an inhibitory effect on both NF-κB activation pathways.

To analyze putative targets of SB203580, which exert a role in NF-κB activation, we studied molecular components regulated by NOD proteins. Activation of NOD, intracellular receptor proteins for bacterial peptidoglycan, plays a crucial role in the pathogenesis of IBD (26) by triggering intestinal inflammation (3–6). RICK is a critical downstream kinase of NOD2 and regulates IKKα finally leading to NF-κB activation (45). Therefore, we assessed RICK activity during our experimental colitis induction. Immunoprecipitated RICK from protein extracts derived from bowel tissue phosphorylates MBP in an in vitro kinase assay (Fig. 5*D*). Those assays indicated that RICK is dramatically activated during development of experimentally induced ulcerative colitis. Activation of RICK can be almost completely inhibited by SB203580 treatment of the mice (Fig. 5*D*). Thus, on the basis of our data, the inhibition of RICK by SB203580 may be responsible for the efficient suppression of NF-κB activation and the release of proinflammatory cytokines.

DISCUSSION

The main goal of this study was to analyze the impact of SB203580 upon inflammation in a murine model of IBD. DSS-induced colitis in Balb/c mice is used as a model system for the respective human inflammatory bowel disease. Crypt abscesses and colitis with epithelial neoplasia leading to colon cancer underline the relevance of this animal model for human ulcerative colitis (7, 8). Further, DSS-induced colitis in mice has a high value in assessing the efficacy of therapeutic agents commonly used in the treatment of colitis. All therapeutically beneficial substances in human IBD were also shown to reduce the disease activity in this mouse model (8, 43, 46, 47). DSS has to be removed after day 7 otherwise mice die due to loss of blood and fluid.

Many lines of evidence suggest that p38 plays a pivotal role in the pathogenesis of IBD. p38 inhibitors are among the most promising substances in the treatment of gastrointestinal inflammation (1, 19). We were able to demonstrate a clinical improvement of DSS-induced colitis as reflected in the DAI and the histological disease score in mice treated with SB203580. Again, the mouse model can be regarded to be accurate for assessing SB203580 effects since clinical improvement induced by this inhibitor started before removal of DSS. However, a recent study did not show uniformly beneficial effects of SB203580 in trinitrobenzene sulfonic acid (TNBS)-induced colitis (23). This might be at least partly due to the inability of SB203580 to inhibit TNF-α synthesis at the rather low concentration used in this study. A second explanation for the differences might be variations in the susceptibilities of different Balb/c mice strains to chemically induced colitis (48).

TNF-α is the most important cytokine in the pathogenesis of IBD, and it is regulated by p38 (49). It has been shown that the AU-rich elements in the 3′ untranslated region of the TNF-α gene are necessary for p38-mediated regulation. Mice develop inflammatory bowel disease and inflammatory arthritis when these AU-rich regions are deleted in the genome resulting in an increased TNF-α expression (50). p38 inhibitors suppress TNF-α synthesis in wild-type mice, whereas AU-rich element deleted mice did not respond to the drug (51). In our experimental model, we could confirm that SB203580 down-regulates TNF-α expression in mice as well as other proinflammatory cytokines with the exception of IL-2 (15, 51–53). In contrast, expression of the anti-inflammatory cytokine IL-10 is up-regulated by SB203580. In general, SB203580 appears to induce an anti-inflammatory response in the inflamed bowel tissue.

We analyzed the impact of SB203580 on p38 MAPK and NF-κB and found that both are dramatically activated during the development of colitis (Fig. 6). As expected, treatment of the mice with SB203580 resulted in a strong inhibition of p38. However, p38 was not the only target of SB203580-mediated inhibition. The colitis-induced activation of NF-κB, a potent transcription factor regulating cellular immune responses and inflammation (31) was also strongly down-regulated by SB203580 treatment. This inhibition was not only observed for the classical NF-κB activation pathway based on the signal-induced proteasomal degradation of the IκBs (54), but was also detected for the more recently discovered so-called alternative mode of NF-κB activation characterized by the NIK/IKKα-mediated processing of the p100 precursor to active p52 (32–34, 55). p100 processing preferentially generates a subset of NF-κB dimers, mainly p52/RelB, distinct from the dimers generated by the classical NF-κB activation. Thus, the

two processes leading to NF-κB activation might have different functions. Recent studies using transgenic mice indicate that the alternative activation pathway of NF-κB initiates immune responses connected to the adaptive immunity, increases chemokine concentrations, and the susceptibility to inflammation in general (35–38). Future studies are necessary to assess the differential contribution of the two activation pathways to IBD pathogenesis.

The finding that the alternative process of NF-κB activation is induced in the course of inflammation associated with IBD and that this activation can be suppressed by SB203580 were unexpected. Another study using epithelial cells demonstrated that SB203580 had no effect on IL-1β-induced NF-κB activation (56). IL-1-triggered NF-κB activation uses intracellular signaling different from the NOD/RICK pathway analyzed in our study. IL-1-receptor-driven signaling involves MyD88 and TRAF6 as the main mediators of intracellular signaling but not NOD. It is very improbable that the inhibitory effects of SB203580 on both NF-κB activation pathways are indirect, for example, mediated by the decrease of cytokines as a result of p38 inhibition. Cytokine synthesis is not regulated by p38 alone. NF-κB is always involved in the regulation of proinflammatory cytokine genes. The more likely explanation would be that SB203580 has a broader range of target protein kinases. Our data strongly suggest that SB203580 directly or indirectly suppresses kinases involved in NF-κB activation. Candidate target protein kinases for such an SB203580-mediated inhibition could be NIK and the IKKs, which are involved in both the classical and the alternative mode of NF-κB activation. As demonstrated in this study, the activity of the IKKs was indeed down-regulated following SB203580 treatment of the mice. One strong candidate for a target of SB203580-mediated inhibition is the serine/threonine protein kinase RICK. We focused our studies on this kinase for three reasons: 1) As shown by a very recent proteome-wide study, RICK is a high-affinity target of SB203580 (57); 2) RICK is known to interact with and activate IKKα (45); and 3) RICK is a prominent effector kinase of NOD proteins (26), which represent intracellular receptors of bacterial peptidoglycan and are assumed to play a pivotal role in IBD pathogenesis (24–26). RICK, like p38 and NF-κB, was strongly activated in the course of experimentally induced colitis, and this activation was also drastically reduced by SB203580 treatment of the mice. Functional studies demonstrate that NOD2 mutations result in failure to activate NF-κB (25). However, experimental evidence that carriers of these NOD2 mutations have decreased NF-κB activation is still lacking. Furthermore, one might assume that different pathogenic pathways contribute to an inappropriate immune response in patients with IBD because the majority of those patients have no such mutations and all patients with IBD have strongly increased NF-κB activation (58). Since RICK is so far the only accepted effector kinase regulated by NOD1 (45), we can assume also an activation of RICK by NOD2 recognizing the homology of NOD1 and NOD2. Our findings indicate that a pathway triggered by bacteria involving NOD proteins as well as RICK, which finally leads to NF-κB activation, might play a pivotal role in IBD pathogenesis. However, further studies are necessary proving the assumption that NOD proteins in ulcerative colitis-associated NF-κB activation are definitively involved. Furthermore, RICK might be a promising new molecular target to inhibit inflammation associated with IBD. Since all conventionally used drugs for anti-inflammatory therapy of ulcerative colitis (aminosalicylate/sulfasalazine, steroids) target NF-κB (59, 60), specific RICK inhibitors might be a new therapeutic option either as primary therapy or as a therapeutic alternative in refractory courses of inflammation after standard therapy. However, the exact molecular signal

transduction sequence(s) leading to NF-κB activation in Crohn's disease and the importance of NOD-associated CARD proteins like RICK are not fully understood so far and need to be further analyzed in future studies.

Taken together, SB203580 reduced the severity of the intestinal inflammation corresponding to improved clinical performance. Investigating the underlying molecular mechanisms, SB203580 was shown to significantly reduce proinflammatory cytokines at the transcriptional level probably due to a significant inhibition of p38 and the classical as well as the alternative pathways of NF-κB activation. The inhibitory effect of SB203580 on NF-κB could be, to a large extent, mediated by RICK inhibition. Therefore, the p38 inhibitor SB203580 is acting on different signal transduction pathways.

ACKNOWLEDGMENTS

The authors thank Christine Wolf for excellent technical assistance and Dr. Jonathan Lindquist for critical reading of the manuscript. The work was supported by a DFG grant NA 292/5-3 to M.N., and by the Magdeburger Forschungsverbund (NBL3) founded by the BMBF with the grants Spitzenbonusprojekt to M.N. and Rotationsstelle to E.H.

REFERENCES

1. Podolsky, D. K. (2002) Inflammatory bowel disease. *N. Engl. J. Med.* **347,** 417–429

2. Bonen, D. K., Ogura, Y., Nicolae, D. L., Inohara, N., Saab, L., Tanabe, T., Chen, F. F., Foster, S. J., Duerr, R. H., Brant, S. R., Cho, J. H., and Nunez, G. (2003) Crohn's disease-associated NOD2 variants share a signaling defect in response to lipopolysaccharide and peptidoglycan. *Gastroenterology* **124**, 140–146

3. Swidsinski, A., Ladhoff, A., Pernthaler, A., Swidsinski, S., Loening-Baucke, V., Ortner, M., Weber, J., Hoffmann, U., Schreiber, S., Dietel, M., et al. (2002) Mucosal flora in inflammatory bowel disease. *Gastroenterology* **122,** 44–54

4. D'Haens, G. R., Geboes, K., Peeters, M., Baert, F., Penninckx, F., and Rutgeerts, P. (1998) Early lesions of recurrent Crohn's disease caused by infusion of intestinal contents in excluded ileum. *Gastroenterology* **114,** 262–267

5. Taurog, J. D., Richardson, J. A., Croft, J. T., Simmons, W. A., Zhou, M., Fernandez-Sueiro, J. L., Balish, E., and Hammer, R. E. (1994) The germ-free state prevents development of gut and joint inflammatory disease in HLA-B27 transgenic rats. *J. Exp. Med.* **180,** 2359–2364

6. Girardin, S. E., Hugot, J. P., and Sansonetti, P. J. (2003) Lessons from Nod2 studies: towards a link between Crohn's disease and bacterial sensing. *Trends Immunol.* **24,** 652–658

7. Okayasu, I., Hatakeyama, S., Yamada, M., Ohkusa, T., Inagaki, Y., and Nakaya, R. (1990) A novel method in the induction of reliable experimental acute and chronic ulcerative colitis in mice. *Gastroenterology* **98,** 694–702

8. Elson, C. O., Sartor, R. B., Tennyson, G. S., and Riddell, R. H. (1995) Experimental models of inflammatory bowel disease. *Gastroenterology* **109,** 1344–1367

9. Axelsson, L. G., Landstrom, E., Goldschmidt, T. J., Gronberg, A., and Bylund-Fellenius, A. C. (1996) Dextran sulfate sodium (DSS) induced experimental colitis in immunodeficient mice: effects in CD4(+)-cell depleted, athymic and NK-cell depleted SCID mice. *Inflamm. Res.* **45,** 181–191

10. Waetzig, G. H., Seegert, D., Rosenstiel, P., Nikolaus, S., and Schreiber, S. (2002) p38 mitogen-activated protein kinase is activated and linked to TNF-alpha signaling in inflammatory bowel disease. *J. Immunol.* **168,** 5342–5351

11. Chang, L., and Karin, M. (2001) Mammalian MAP kinase signalling cascades. *Nature* **410,** 37–40

12. Kyriakis, J. M., and Avruch, J. (1996) Sounding the alarm: protein kinase cascades activated by stress and inflammation. *J. Biol. Chem.* **271,** 24,313–24,316

13. Platanias, L. C. (2003) The p38 mitogen-activated protein kinase pathway and its role in interferon signaling. *Pharmacol. Ther.* **98,** 129–142

14. Zhao, M., New, L., Kravchenko, V. V., Kato, Y., Gram, H., Di Padova, F., Olson, E. N., Ulevitch, R. J., and Han, J. (1999) Regulation of the MEF2 family of transcription factors by p38. *Mol. Cell. Biol.* **19,** 21–30

15. Wysk, M., Yang, D. D., Lu, H. T., Flavell, R. A., and Davis, R. J. (1999) Requirement of mitogen-activated protein kinase kinase 3 (MKK3) for tumor necrosis factor-induced cytokine expression. *Proc. Natl. Acad. Sci. USA* **96,** 3763–3768

16. Lu, H. A. T., Yang, D. D., Wysk, M., Gatti, E., Mellman, I., Davis, R. J., and Flavell, R. A. (1998) Defective IL-12 production in mitogen-activated protein (MAP) kinase kinase 3 (MKK3)-deficient mice. *EMBO J.* **17,** 2817–2829

17. Hampe, J., Shaw, S. H., Saiz, R., Leysens, N., Lantermann, A., Mascheretti, S., Lynch, N. J., MacPherson, A. J., Bridger, S., van Deventer, S., et al. (1999) Linkage of inflammatory bowel disease to human chromosome 6p. *Am. J. Hum. Genet.* **65,** 1647–1655

18. Hu, M. C. T., Wang, Y., Mikhail, A., Qiu, W. R., and Tan, T. H. (1999) Murine p38-δ mitogen-activated protein kinase, a developmentally regulated protein kinase that is activated by stress and proinflammatory cytokines. *J. Biol. Chem.* **274,** 7095–7102

19. Hommes, D., van den Blink, B., Plasse, T., Bartelsman, J., Xu, C., Macpherson, B., Tytgat, G., Peppelenbosch, M., and van Deventer, S. (2002) Inhibition of stress-activated MAP kinases induces clinical improvement in moderate to severe Crohn's disease. *Gastroenterology* **122,** 7–14

20. Waetzig, G. H., and Schreiber, S. (2003) Review article: mitogen-activated protein kinases in chronic intestinal inflammation - targeting ancient pathways to treat modern diseases. *Aliment. Pharmacol. Ther.* **18,** 17–32

21. Badger, A. M., Bradbeer, J. N., Votta, B., Lee, J. C., Adams, J. L., and Griswold, D. E. (1996) Pharmacological profile of SB 203580, a selective inhibitor of cytokine suppressive binding protein/p38 kinase, in animal models of arthritis, bone resorption, endotoxin shock and immune function. *J. Pharmacol. Exp. Ther.* **279,** 1453–1461

22. Nick, J. A., Young, S. K., Brown, K. K., Avdi, N. J., Arndt, P. G., Suratt, B. T., Janes, M. S., Henson, P. M., and Worthen, G. S. (2000) Role of p38 mitogen-activated protein kinase in a murine model of pulmonary inflammation. *J. Immunol.* **164,** 2151–2159

23. Ten Hove, T., van den Blink, B., Pronk, I., Drillenburg, P., Peppelenbosch, M. P., and van Deventer, S. J. H. (2002) Dichotomal role of inhibition of p38 MAPK with SB 203580 in experimental colitis. *Gut* **50,** 507–512

24. Hugot, J. P., Chamaillard, M., Zouali, H., Lesage, S., Cezard, J. P., Belaiche, J., Almer, S., Tysk, C., O'Morain, C. A., Gassull, M., et al. (2001) Association of NOD2 leucine-rich repeat variants with susceptibility to Crohn's disease. *Nature* **411,** 599–603

25. Ogura, Y., Bonen, D. K., Inohara, N., Nicolae, D. L., Chen, F. F., Ramos, R., Britton, H., Moran, T., Karaliuskas, R., Duerr, R. H., et al. (2001) A frameshift mutation in NOD2 associated with susceptibility to Crohn's disease. *Nature* **411,** 603–606

26. Inohara, N., Ogura, Y., and Nunez, G. (2002) Nods: a family of cytosolic proteins that regulate the host response to pathogens. *Curr. Opin. Microbiol.* **5,** 76–80

27. Brant, S. R., Picco, M. F., Achkar, J. P., Bayless, T. M., Kane, S. V., Brzezinski, A., Nouvet, F. J., Bonen, D., Karban, A., Dassopoulos, T., et al. (2003) Defining complex contributions of NOD2/CARD15 gene mutations, age at onset, and tobacco use on Crohn's disease phenotypes. *Inflamm. Bowel Dis.* **9,** 281–289

28. Hampe, J., Grebe, J., Nikolaus, S., Solberg, C., Croucher, P. J., Mascheretti, S., Jahnsen, J., Moum, B., Klump, B., Krawczak, M., et al. (2002) Association of NOD2 (CARD 15) genotype with clinical course of Crohn's disease: a cohort study. *Lancet* **359,** 1661–1665

29. Andriulli, A., Annese, V., Latiano, A., Calmieri, O., Fortina, P., Ardizzone, S., Cottone, M., D'Inca, R., and Riegler, G. (2004) The frame-shift mutation of the NOD2/CARD15 gene is significantly increased in ulcerative colitis: an *IG-IBD study. *Gastroenterology* **126,** 625–627

30. Hisamatsu, T., Suzuki, M., Reinecker, H. C., Nadeau, W. J., McCormick, B. A., and Podolsky, D. K. (2003) CARD15/NOD2 functions as an antibacterial factor in human intestinal epithelial cells. *Gastroenterology* **124,** 993–1000

31. Karin, M., and Lin, A. (2002) NF-κB at the crossroads of life and death. *Nat. Immunol.* **3,** 221–227

32. Senftleben, U., Cao, Y., Xiao, G., Greten, F. R., Krahn, G., Bonizzi, G., Chen, Y., Hu, Y., Fong, A., Sun, S. C., et al. (2001) Activation by IKKα of a second, evolutionary conserved, NF-κB signalling pathway. *Science* **293,** 1495–1499

33. Xiao, G., Harhaj, E. W., and Sun, S. C. (2001) NF-κB-inducing kinase regulates the processing of NF-κB2 p100. *Mol. Cell* **7,** 401–409

34. Claudio, E., Brown, K., Park, S., Wang, H., and Siebenlist, U. (2002) BAFF-induced NEMO-independent processing of NF-κB2 in maturing B cells. *Nat. Immunol.* **3,** 958–965

35. Weih, D. S., Yilmaz, Z. B., and Weih, F. (2001) Essential role of RelB in germinal center and marginal zone formation and proper expression of homing chemokines. *J. Immunol.* **167,** 1909–1919

36. Weih, F., and Caamano, J. (2003) Regulation of secondary lymphoid organ development by the nuclear factor-kappaB signal transduction pathway. *Immunol. Rev.* **195,** 91–105

37. Weih, F., Warr, G., Yang, H., and Bravo, R. (1997) Multifocal defects in immune responses in RelB-deficient mice. *J. Immunol.* **158,** 5211–5218

38. Weih, F., Carrasco, D., Durham, S. K., Barton, D. S., Rizzo, C. A., Ryseck, R. P., Lira, S. A., and Bravo, R. (1995) Multiorgan inflammation and hematopoietic abnormalities in mice with targeted disruption of RelB, a member of the NF-κB/Rel family. *Cell* **80,** 331–340

39. Hartmann, G., Bidlingmaier, C., Siegmund, B., Albrich, S., Schulze, J., Tschoep, K., Eigler, A., Lehr, H. A., and Endres, S. (2000) Specific type IV phosphodiesterase inhibitor rolipram mitigates experimental colitis in mice. *J. Pharmacol. Exp. Ther.* **292,** 22–30

40. Dieleman, L. A., Palmen, M. J., Akol, H., Bloemena, E., Pena, A. S., Meuwissen, S. G., and van Rees, E. P. (1998) Chronic experimental colitis induced by dextran sulphate sodium (DSS) is characterized by Th1 and Th2 cytokines. *Clin. Exp. Immunol.* **114,** 385–391

41. Wex, T., Treiber, G., Lendeckel, U., and Malfertheiner, P. (2003) A two-step method for the extraction of high-quality RNA from endoscopic biopsies. *Clin. Chem. Lab. Med.* **41,** 1033–1037

42. Naumann, M., and Scheidereit, C. (1994) Activation of NF-κB in vivo is regulated by multiple phosphorylations. *EMBO J.* **13,** 4597–4607

43. Murthy, S. N., Cooper, H. S., Shim, H., Shah, R. S., Ibrahim, S. A., and Sedergran, D. J. (1993) Treatment of dextran sulfate sodium-induced murine colitis by intracolonic cyclosporin. *Dig. Dis. Sci.* **38,** 1722–1734

44. Young, J., Mc Laughlin, M. M., Kumar, S., Kassis, S., Doyle, M. L., McNulty, D., Gallagher, T. F., Fisher, S., McDonnell, P. C., Carr, S. A., et al. (1997) Pyridinyl imidazol inhibitors of p38 mitogen-activated protein kinase bind in the ATP site. *J. Biol. Chem.* **272,** 12,116–12,121

45. Girardin, S. E., Tournebize, R., Mavris, M., Page, A. L., Li, X., Stark, G. R., Bertin, J., DiStefano, P. S., Yaniv, M., Sansonetti, P. J., et al. (2001) CARD4/Nod1 mediates NF-kappaB and JNK activation by invasive *Shigella flexneri*. *EMBO Rep.* **2,** 736–742

46. Kojouharoff, G., Hans, W., Obermeier, F., Mannel, D. N., Andus, T., Scholmerich, J., Gross, V., and Falk, W. (1997) Neutralization of tumour necrosis factor (TNF) but not of IL-1 reduces inflammation in chronic dextran sulphate sodium-induced colitis in mice. *Clin. Exp. Immunol.* **107,** 353–358

47. Axelsson, L. G., Landstrom, E., and Bylund-Fellenius, A. C. (1998) Experimental colitis induced by dextran sulphate sodium in mice: beneficial effects of sulphasalazine and olsalazine. *Aliment. Pharmacol. Ther.* **12,** 925–934

48. Beagley, K. W., Black, C. A., and Elson, C. O. (1991) Strain differences in susceptibility to TNBS-induced colitis. *Gastroenterolgy* **100,** A560

49. Kyriakis, J. M., and Avruch, J. (2001) Mammalian mitogen-activated protein kinase signal transduction pathways activated by stress and inflammation. *Physiol. Rev.* **81,** 807–869

50. Kontoyiannis, D., Pasparakis, M., Pizarro, T. T., Cominelli, F., and Kollias, G. (1999) Impaired on/off regulation of TNF biosynthesis in mice lacking TNF AU rich elements: implications for joint and gut-associated immunopathologies. *Immunity* **10,** 387–398

51. Kontoyiannis, D., Kotlyarov, A., Carballo, E., Alexopoulou, L., Blackshear, P. J., Gaestel, M., Davis, R., Flavell, R., and Kollias, G. (2001) Interleukin-10 targets p38 MAPK to modulate ARE-dependent TNF mRNA translation and limit intestinal pathology. *EMBO J.* **20,** 3760–3770

52. Rincon, M., Enslen, H., Raingeraud, J., Recht, M., Zapton, T., Su, M. S., Penix, L. A., Davis, R. J., Flavell, R. A., et al. (1998) Interferon-gamma expression by Th1 effector T cells mediated by the p38 MAP kinase signaling pathway. *EMBO* **17,** 2817–2829

53. Lu, H. T., Yang, D. D., Wysk, M., Gatti, E., Mellman, I., Davis, R. J., and Flavell, R. A. (1999) Defective IL-12 production in mitogen-activated protein (MAP) kinase kinase 3 (Mkk3)-deficient mice. *EMBO J.* **18,** 1845–1857

54. Karin, M., and Ben-Neriah, Y. (2000) Phosphorylation meets ubiquitination: the control of NF-κB activity. *Annu. Rev. Immunol.* **18,** 621–663

55. Pomerantz, J. L., and Baltimore, D. (2002) Two Pathways to NF-κB. *Mol. Cell* **10,** 693–695

56. Parhar, K., Ray, A., Steinbrecher, U., Nelson, C., and Salh, B. (2003) The p38 mitogen-activated protein kinase regulates interleukin-1beta-induced IL-8 expression via an effect on the IL-8 promoter in intestinal epithelial cells. *Immunology* **108,** 502–512

57. Godl, K., Wissing, J., Kurtenbach, A., Habenberger, P., Blencke, S., Gutbrod, H., Salassidis, K., Stein-Gerlach, M., Missio, A., Cotten, M., et al. (2003) An efficient proteomics method

to identify the cellular targets of protein kinase inhibitors. *Proc. Natl. Acad. Sci. U.S.A.* **100,** 15,434–15,439

58. Neurath, M. F., Fuss, I., Schurmann, G., Pettersson, S., Arnold, K., Muller-Lobeck, H., Strober, W., Herfarth, C., and Buschenfelde, K. H. (1998) Cytokine gene transcription by NF-kappa B family members in patients with inflammatory bowel disease. *Ann. N. Y. Acad. Sci.* **859,** 149–159

59. Daperno, M., Sostegni, R., Rocca, R., Rigazio, C., Scaglione, N., Castellino, F., Ercole, E., and Pera, A. (2002) Review article: medical treatment of severe ulcerative colitis. *Aliment. Pharmacol. Ther.* **16, Suppl 4,** 7–12

60. Gionchetti, P., Amadini, C., Rizzello, F., Venturi, A., and Campieri, M. (2002) Review article: treatment of mild to moderate ulcerative colitis and pouchitis. *Aliment. Pharmacol. Ther.* **16, Suppl 4,** 13–19

Received March 25, 2004; accepted June 18, 2004.

Fig. 1

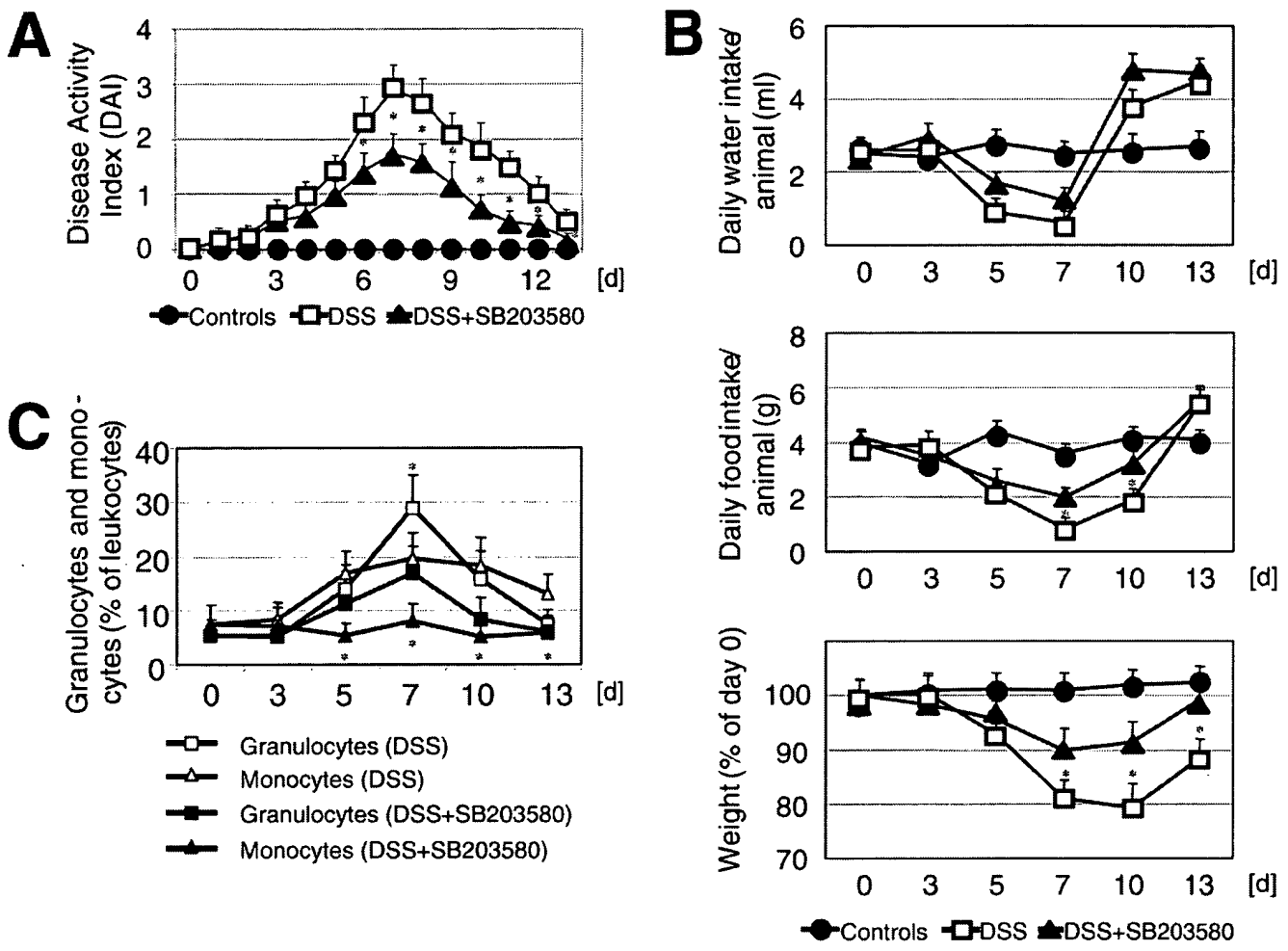

Figure 1. Effect of SB203508 on DSS-induced colitis. ***A)*** Colitis was induced in Balb/c mice by oral administration of 3% DSS for 7 days followed by a 6-day observation period. Values are means ± SD of 7 animals/group/day. Results for DSS-administered mice with SB203508 treatment were compared with mice without SB203580 treatment (**P*<0.05). ***B)*** Schematic presentation of daily water and food intake as well as weight loss of the mice over the experimental period. Values are means ± SD of 7 animals/group/day. Results for DSS-administered mice with SB203508 treatment were compared with mice without SB203580 treatment (**P*<0.05). ***C)*** Differential blood cell counts were measured after intracardially drawn blood immediately obtained after sacrifice. Values are means ± SD of 7 animals/group/day. Results for DSS-administered mice with SB203508 treatment were compared with mice without SB203580 treatment (**P*<0.05).

Fig. 2

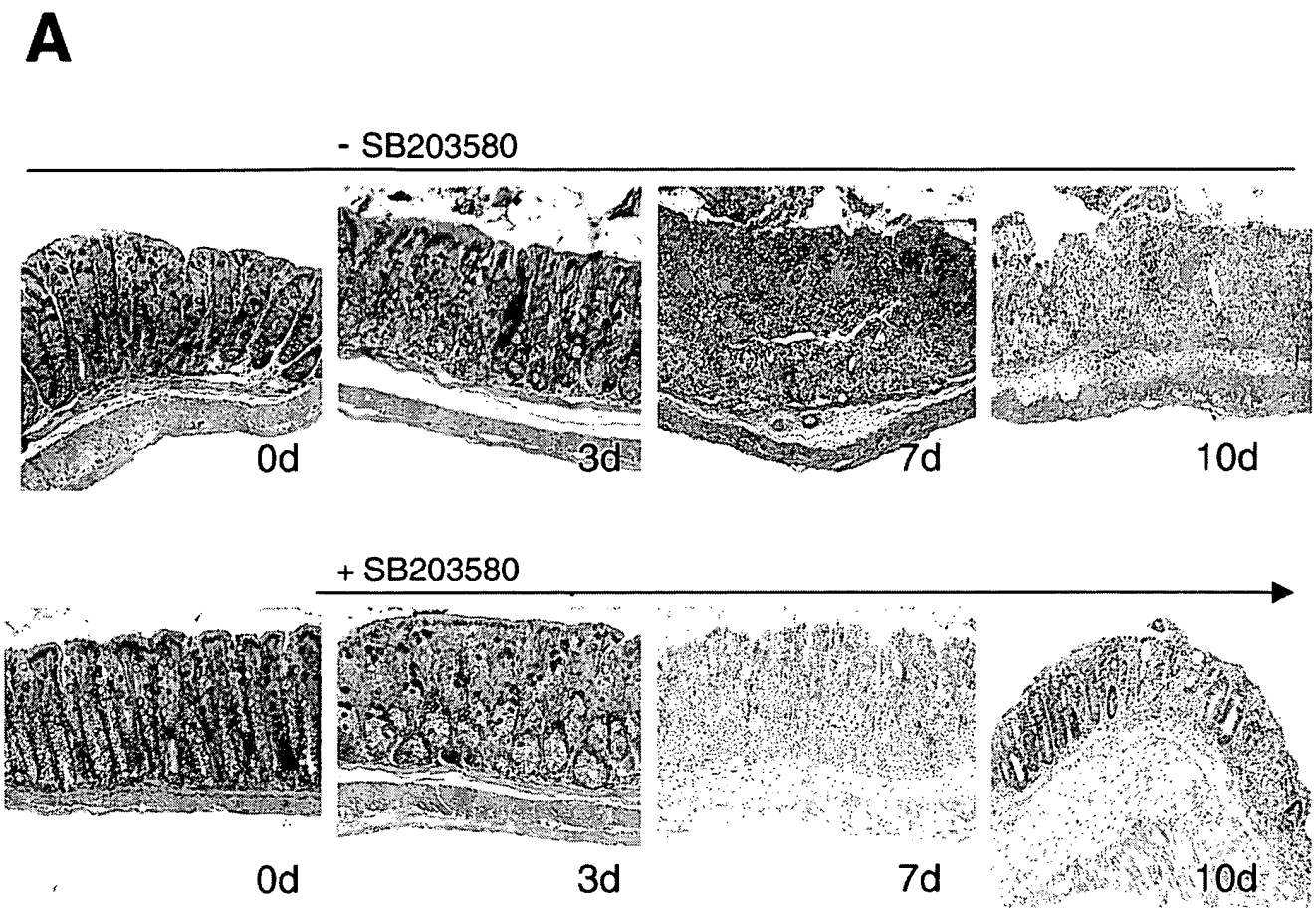
A
- SB203580
0d
3d
7d
10d
+ SB203580
0d
3d
7d
10d
B
Histological Score
40
30
20
10
0
0 3 5 7 10 13 [d]
Controls
DSS
DSS+SB203580

Figure 2. Influence of SB203580 on histological alterations in DSS-induced colitis. ***A***) Bowel tissue from Balb/c mice after DSS-induced colitis without (***upper panel***) and with SB203580 administration (***lower panel***) were fixed in 3% formaldehyde and stained with hematoxylin/eosin (HE). The DSS-induced damages of the mucosa in mice not treated with SB203580 were seen starting at day 3 and showing extensive ulcerations at day 7. DSS administration was discontinued after day 7 resulting in a resolution of inflammatory infiltrates mainly associated with a diffuse infiltration of mononuclear cells, plasma cells, and granulocytes. Treatment with SB203508 reduced mucosal injury, edema, and infiltration of inflammatory cells in the colonic bowel. The histology of the distal large intestine in the control group without and with daily i.p.-injections of SB 203508 revealed normal. (HE-staining, magnification ×20). ***B***) Histological scoring was performed semiquantitatively in HE-stained sections. Values are means ± SD of 7 animals/group/day. Results for DSS-administered mice with SB203508 treatment were compared with mice without SB 203580 treatment (*P<0.05).

Fig. 3

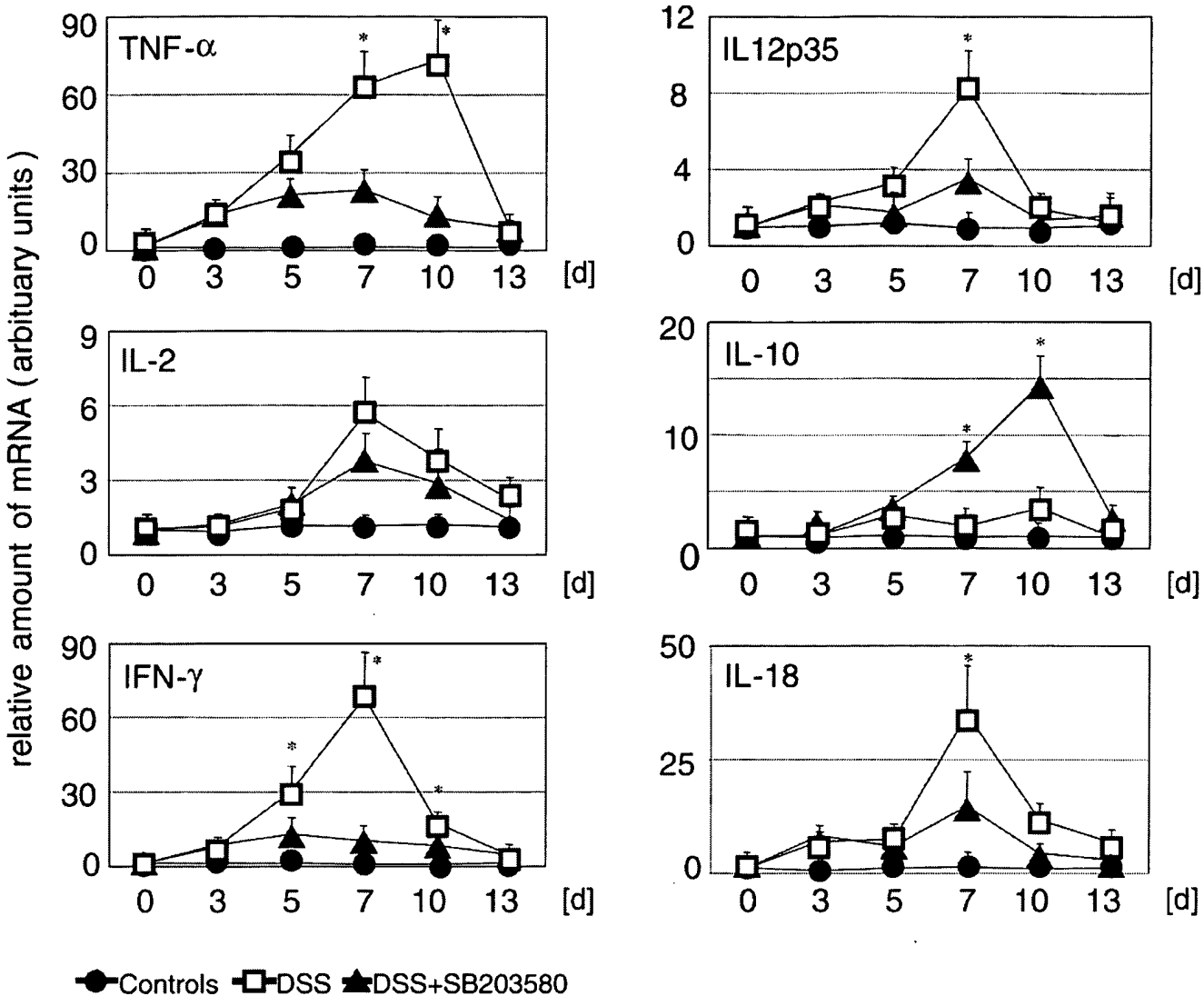

Figure 3. SB203580 inhibits proinflammatory cytokine mRNA expression. Descendent colon was removed from untreated mice (control), DSS-fed, and DSS-fed plus SB203580-treated mice. The tissue was homogenized in Trizol as described in Materials and Methods. Amounts of colonic cytokine mRNAs were quantified using real-time RT-PCR. Values are means ± SE (n=7 mice/group/day, *P<0.05 DSS-fed mice with vs. without SB 203580 treatment).

Fig. 4

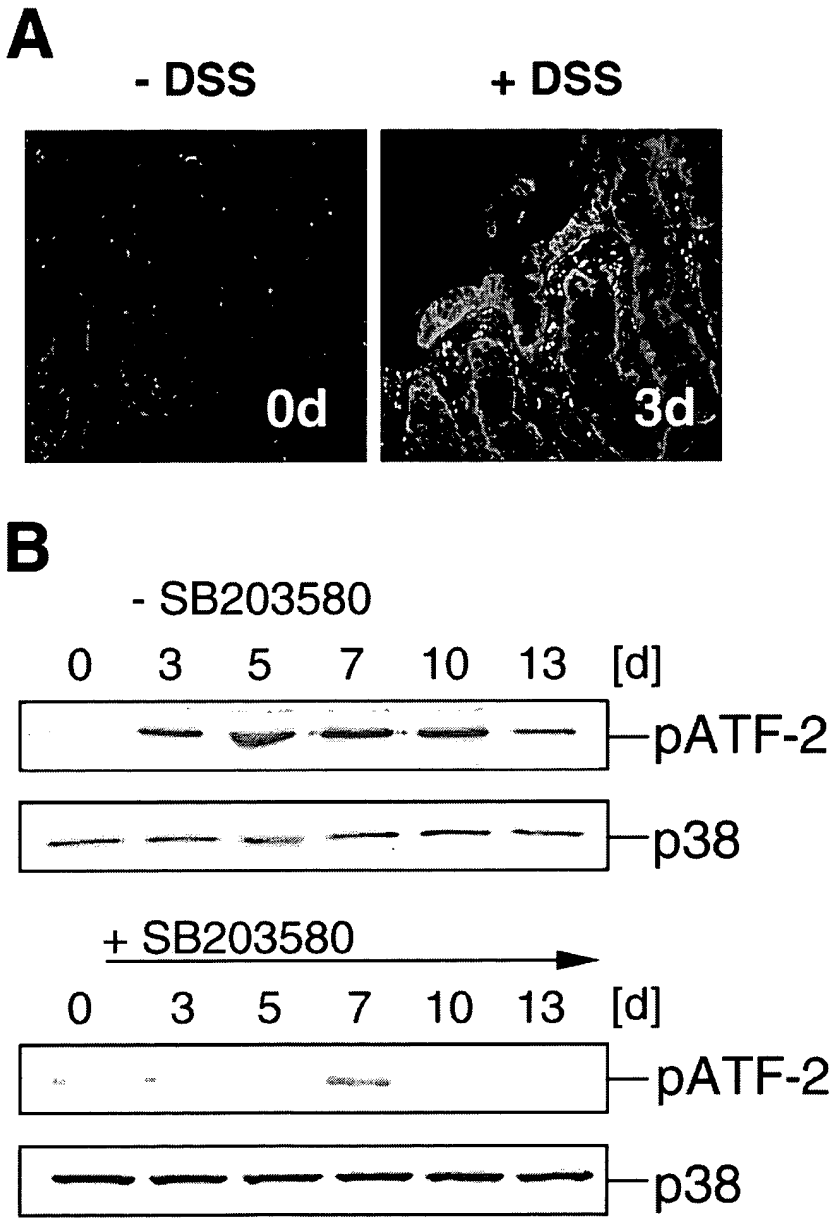

Figure 4. SB203580 inhibits p38 activation in mononuclear- and plasma cells. ***A***) Immunofluorescence microscopy of the descendent colon was performed using FITC-coupled phospho-specific antibodies against p38 (see Materials and Methods) in non-DSS exposed animals (left/0d) and in mice fed with DSS for 3 days (right/3d). p38 activity was only observed in mononuclear- and plasma cells of the lamina propria. ***B***) p38 was immunoprecipitated from protein extracts of the descendent colon of untreated (control) or DSS-fed Balb/c mice that were either pretreated with SB203580 or left untreated (n=7 mice/group/day). The immunocomplexes were subjected to an in vitro kinase assay using ATF-2 as substrate followed by immunoblotting with an anti-phospho-ATF-2 antibody. To control equal loading, immunoblotting with p38-specific antibodies was performed. All results are representative of three independent experiments.

Fig. 5

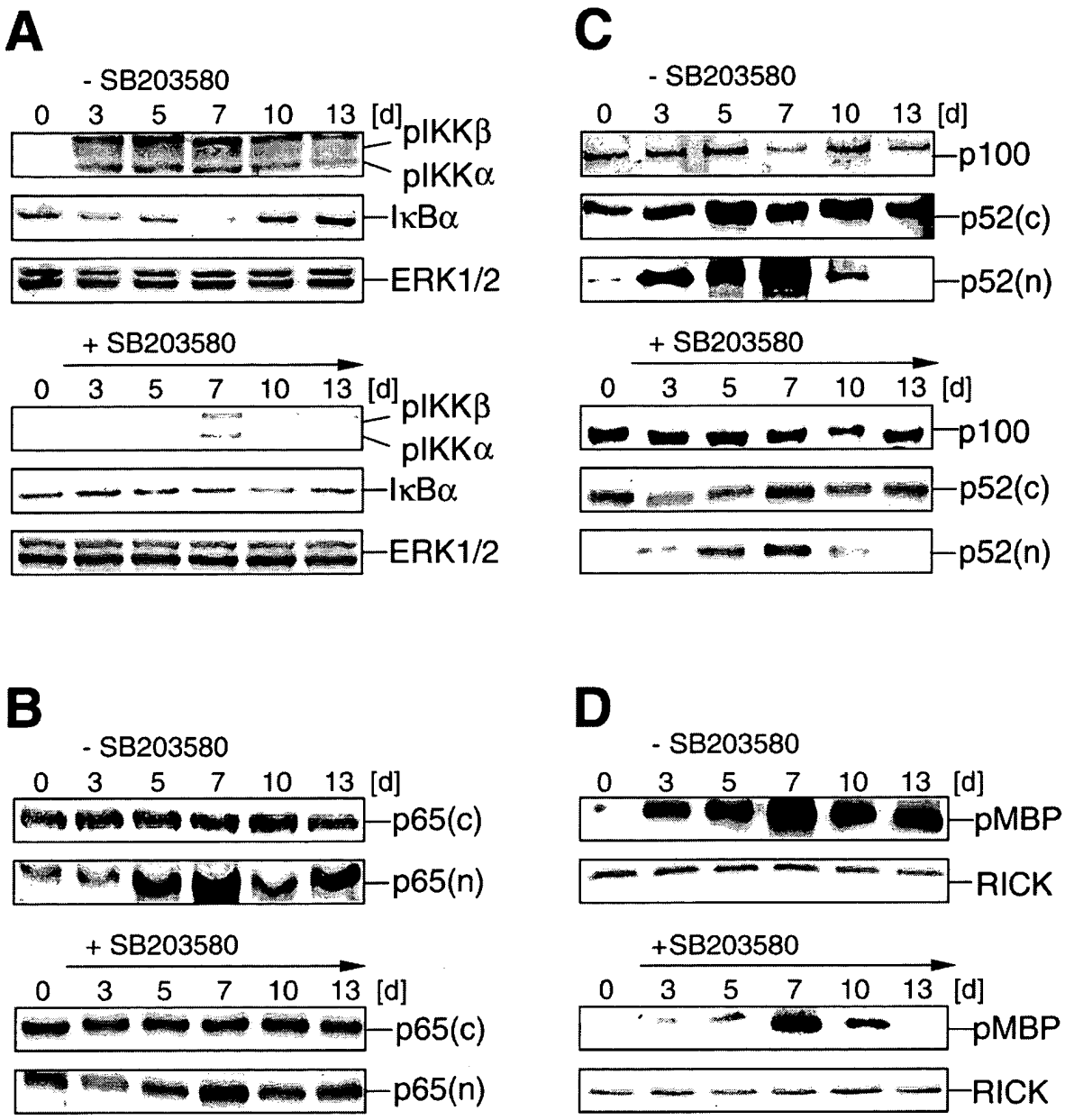

Figure 5. SB203580 inhibits NF-κB and RICK in DSS-induced colitis. ***A***) Protein extracts from the bowel of DSS-treated Balb/c mice were analyzed by immunoblotting using phospho-specific IKK and IκBα antibodies. Mice (n=7 mice/group/day) were either left untreated or administered with SB203580 for the indicated time. To control equal loading, blots were reprobed with ERK 1/2 antibody. Cytoplasmic (c) and nuclear (n) protein extracts were prepared from bowel tissue and immunoblotted with p65 (***B***) or p100/p52 specific antibodies (***C***). Protein concentration was measured for the subcellular protein extracts as described in Materials and Methods. Additionally, the filters were reprobed with an ERK1/2 antibody as a loading control (data not shown). (***D***) RICK was immunoprecipitated with RICK-specific antibody from whole cellular extracts of bowel tissue from DSS-fed Balb/c mice which were either treated or untreated with SB203580 (n=7 mice/group/day). The immunocomplexes were subjected to an in vitro kinase assay using MBP as substrate for RICK-dependent phosphorylation followed by immunoblotting with antiphospho-MBP antibody. To control equal loading, the blots were reprobed with RICK antibody. All results are representative of three independent experiments.

Fig. 6

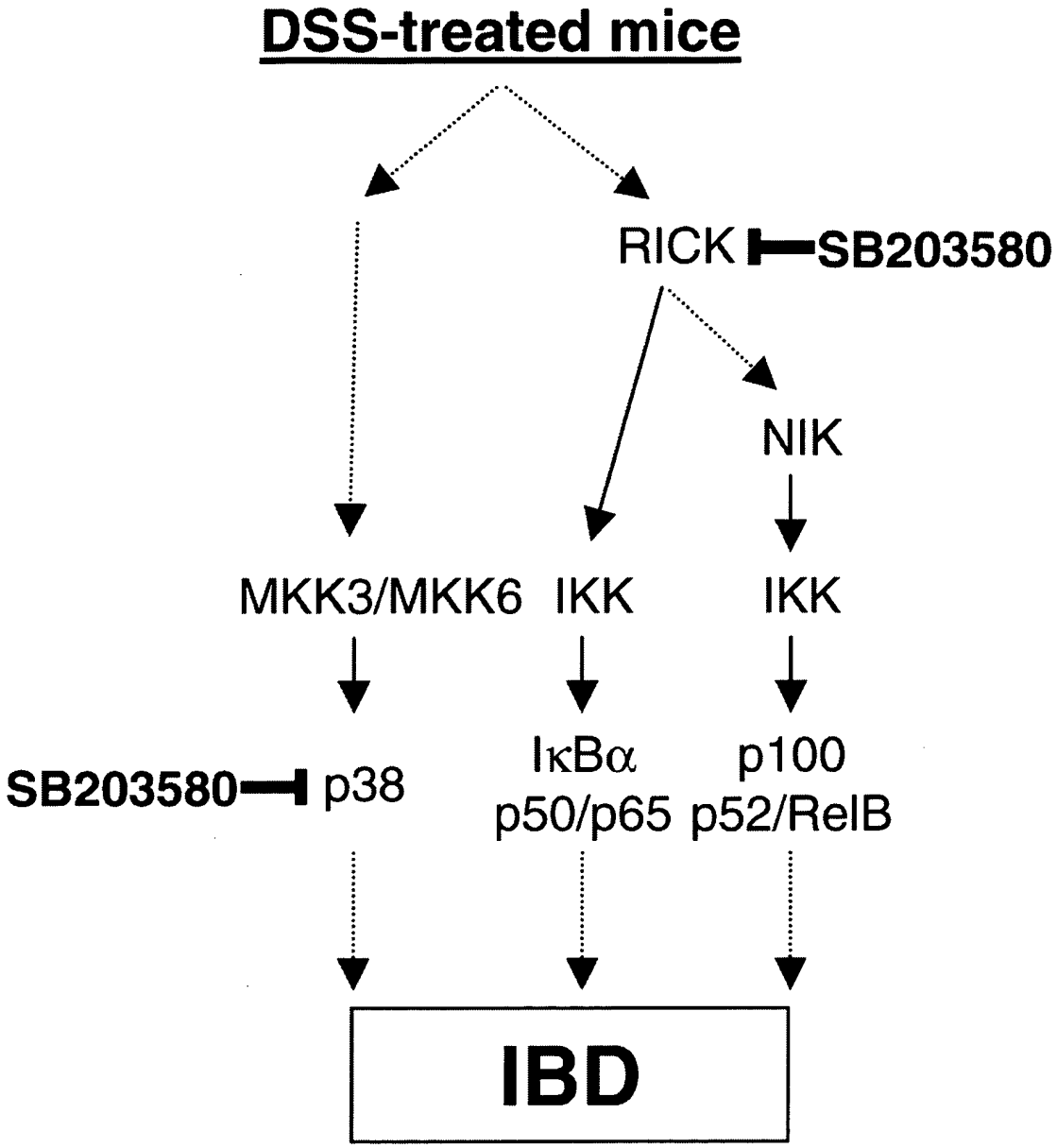

Figure 6. Schematic model of inflammatory pathways inhibited by SB203580. Oral administration of DSS induces ulcerative colitis in mice. This triggers p38 MAPK activity via the upstream kinases MKK3/6 and NF-κB activation via the "classical" IκB-dependent and "alternative" pathway based on processing of p100. The activation of both pathways is mediated by the IKK complex. RICK is a kinase upstream of IKK, which is able to activate the IKK complex. RICK activity is also induced upon colitis induction. SB203580 inhibits p38 MAPK, as well as RICK activity. Suppression of RICK leads to down-regulation of NF–κB. The solid arrows indicate direct activation of downstream targets, and the dotted arrows indicate indirect or not yet defined activation processes.